OFDM SYNCHRONIZATION SCHEME TO BE USED ON A NON FREQUENCY SELECTIVE SATELLITE CHANNEL

Anh Tai Ho[(1)], *Marie-Laure Boucheret*[(1)], *Nathalie Thomas*[(1)], *Mathieu Dervin*[(3)], *Xavier Deplancq*[(2)]

[(1)] University of Toulouse, IRIT/ENSEEIHT/TéSA, 2 rue Camichel, 31071 Toulouse, France
[(2)] CNES, 18 av. Edouard Belin, 31401 Toulouse Cedex 4, France
[(3)] Thales Alenia Space, 26 av Jean François Champollion, BP 33787, 31037 Toulouse Cedex 1, France
Phone : (+33) 0561588011, fax : (+33) 0561247373
Emails : anh-tai.ho@tesa.prd.fr, xavier.deplancq@cnes.fr
{marie-laure.boucheret,nathalie.thomas}@n7.fr, mathieu.dervin@thalesaleniaspace.com

ABSTRACT

This paper proposes an OFDM receiver for the forward link of a fixed broadband satellite system. We focus on the synchronization tasks in the receiver. Our objective is to reduce to the minimum the needed overhead, in order to improve spectral efficiency compared to a single carrier waveform system. A non pilot aided algorithm is used. However it is preceded by a coarse synchronization stage, in which a limited overhead is necessary (short cyclic prefix associated to a few number of pilots). The performance of the proposed receiver is assessed through several simulation results.

1. INTRODUCTION

Orthogonal Frequency Division Multiplexing (OFDM) waveform is widely used for high data rate transmissions over frequency selective channels, such as terrestrial digital video broadcasting or wireless local and metropolitan area networks. Even if the satellite channel is not frequency selective, OFDM could be preferred to single carrier waveforms if it allows to improve the system spectral efficiency. The gain arises from the possibility to reduce the overhead in a non-frequency selective channel. Indeed, a large part of the overhead in OFDM-based terrestrial systems is introduced so as to face up to the channel frequency selectivity: guard interval to cancel the inter-symbol interference induced by multi-path, pilot symbols to perform channel equalization in the receiver. However, a part of the overhead is still necessary in a non-frequency selective channel in order to perform synchronization in the receiver. The purpose of this paper is to investigate an OFDM waveform receiver needing the lightest possible overhead, to be used on the forward link of a fixed broadband satellite system. In the literature, some complete receiver structures are proposed for fixed and mobile terrestrial channels [1] [2]. Besides, many algorithms for timing and frequency recovery are investigated [3] [4] [5]. Based on these proposals, we propose in this work to maintain a limited pilot overhead and short cyclic prefix in order to allow coarse symbol timing and carrier frequency synchronization. Then for fine synchronization, non pilot aided loop structures are defined. No channel equalization is required in this context. The performance of the receiver is assessed by simulation.

2. PROBLEM FORMULATION

We consider an OFDM waveform with N QPSK modulated subcarriers. The i-th OFDM symbol is composed of N samples, obtained from inverse Fast Fourier Transform (iFFT) computed on the i-th block of N information symbols to be transmitted: $\{\sum_{n=0}^{N-1} X_{i,n} e^{j2\pi \frac{nm}{N}}\}_{m=0,\ldots,N-1}$. $X_{i,n}$ denotes the QPSK information symbol mapped on the n-th subcarrier in the i-th OFDM symbol. A cyclic prefix (CP) of N_p samples is classically inserted at the beginning of each OFDM symbol to suppress Inter Symbol Interference (ISI) in terrestrial channels [1]. We propose to keep it in our receiver in order to conduct the coarse synchronization stage.

At the output of the satellite transmission channel, the signal is corrupted by additive white gaussian noise (AWGN). Received symbols can be written as: $Y_{i,n} = X_{i,n} + w_{i,n}$, where $w_{i,n}$ is an AWGN noise sample. In the receiver the cyclic prefix is removed and a N bin FFT is applied to the sampled signal in order to recover the information on the subcarriers. However, some synchronization impairments may appear:

- An error in the FFT window positioning, defined as the number of samples separating the first of the N received samples processed in the FFT, from the effective beginning of the corresponding OFDM symbol. This error is called symbol timing error and is denoted τ.
- A sampling clock frequency error, referred to as β after normalization to the OFDM symbol rate.
- A carrier frequency error. This error is normalized to the subcarrier spacing and denoted Δf.
- A carrier phase error ϕ, at a reference time instant.

The impact of each synchronization error on the received symbols is described in this section.

2.1 Effects of symbol timing error

The condition $-Np < \tau \leq 0$ guaranties, after the FFT, the absence of inter symbol interference. In that case τ only involves a phase rotation on each subcarrier [6]:

$$Y_{i,n} = \exp\left(\frac{j2\pi n\tau}{N}\right) X_{i,n} + w_{i,n}. \quad (1)$$

Otherwise, received symbols can be written as:

$$Y_{i,n} = \frac{N - |\tau|}{N} \exp\left(\frac{j2\pi n\tau}{N}\right) X_{i,n} + I_{\tau,n} + w_{i,n}, \quad (2)$$

where $I_{\tau,n}$ denotes the Inter Symbol Interference (ISI) depending on τ and n.

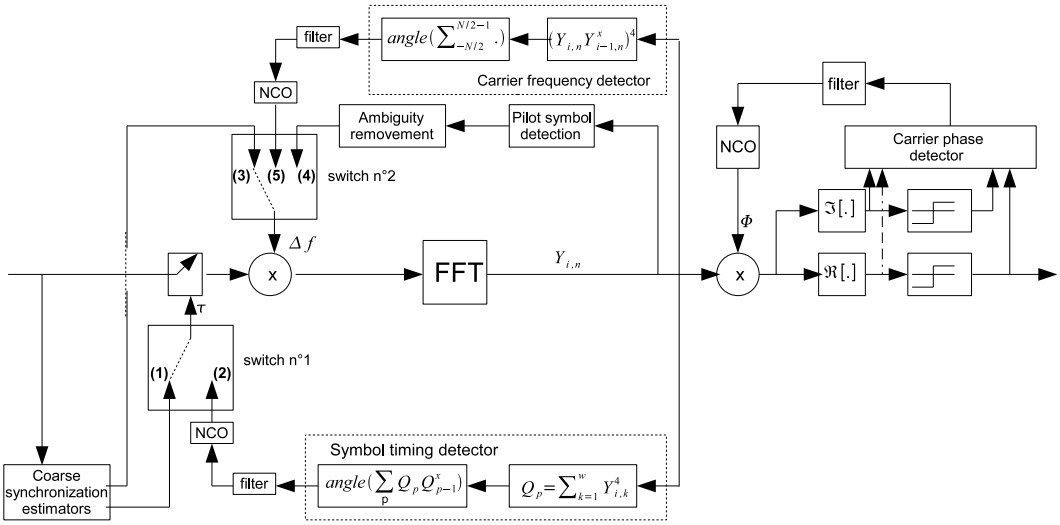

Figure 1: Proposed receiver structure for synchronization

2.2 Effects of clock frequency error

The clock frequency error β leads to the following distortion on the received symbols [6]:

$$Y_{i,n} = \exp\left[j2\pi\left(i-\frac{1}{2}\right)n\beta\right]\frac{\sin(\pi n\beta)}{\pi n\beta}X_{i,n} + I_{\beta,n} + w_{i,n}, \quad (3)$$

where $I_{\beta,n}$ is an inter carrier interference term (ICI), with zero mean and a variance equal to: $var[I_{\beta,n}] = \frac{\pi^2}{3}(n\beta)$.

2.3 Effects of carrier phase and frequency errors

Carrier phase error ϕ introduces a constant rotation on the received symbols:

$$Y_{i,n} = \exp(j\phi)X_{i,n} + w_{i,n}. \quad (4)$$

On the other hand, a carrier frequency error Δf breaks the orthogonality between subcarriers introducing some Inter Carrier Interference (ICI) [7]:

$$Y_{i,n} = \exp\left[j2\pi\left(i-\frac{1}{2}\right)\Delta fT\right]\frac{sin(\pi\Delta fT)}{\pi\Delta fT}X_{i,n} + I_{\Delta f,n} + w_{i,n}. \quad (5)$$

$I_{\Delta f,n}$ is the ICI term depending on Δf and n and T stands for the OFDM symbol duration.

2.4 Overall effect of synchronization impairments

The cumulated effects of all possible synchronization errors: τ, Δf, β and ϕ, leads to the following expression of the received symbols:

$$Y_{i,n} = A\exp(j\theta_{i,n})X_{i,n} + I_{i,n} + w_{i,n}, \quad (6)$$

where $I_{i,n}$ denotes the overall interference term, A refers to the overall attenuation and $\theta_{i,n}$ is the overall rotation. All these terms depend on τ, Δf, β and ϕ. Assuming that τ, Δf, β and ϕ are independent (assessed by simulations), $\theta_{i,n}$ can be written as:

$$\theta_{i,n} = \phi + \frac{2\pi n\tau}{N} + 2\pi(i-1/2)\Delta fT + 2\pi(i-1/2)n\beta \quad (7)$$

3. PROPOSED RECEIVER

3.1 Overall structure

The proposed receiver structure is displayed on figure 1. It is organized in two stages.

A coarse synchronization step is required in order to retrieve the subcarriers at the FFT output without ambiguity, and reduce the interference term $I_{i,n}$ defined in (6). It is detailed in section 3.2.

Relying on this coarse synchronization, non data aided algorithms involving feedback retroaction allow to track the residual timing and carrier frequency errors with more accuracy. Finally, the remaining carrier phase error is corrected on all subcarriers, as described in section 3.3.

The sampling clock frequency error is very low in the considered satellite systems ($\beta < 10^{-5}$). For that reason there is no requirement for a specific synchronization block to recover β. However, it leads to a drift of OFDM symbol timing which has to be taken into account.

The synchronization is performed as the following:

- First, the switch number 1 (S1) is turned to position (1) and the switch number 2 (S2) is turned to position (3). The coarse synchronization stage is activated in order to roughly correct symbol timing and carrier frequency errors.
- Then, S2 is switched to position (4) in order to detect and remove the ambiguity on the carrier frequency error.
- Finally, S1 and S2 are respectively switched to positions (2) and (5) in order to activate fine synchronization stage.

3.2 Coarse synchronization

The cyclic prefix, inserted at the beginning of each OFDM symbol, is a copy of its last N_p samples. This redundancy may be used to provide a first estimation of the symbol timing and carrier frequency errors [8]. A sliding cross correlation function $R(k)$ is computed on the sampled down-converted received signal denoted $r(k)$, for each received

sample:

$$R(k) = \sum_{l=0}^{N_p-1} r^*(k+l)r(k+l+N).$$

$$R(k+1) = R(k) + r^*(k+N_p)r(k+N_p+N) - r^*(k)r(k+N).$$

Observed peaks allow to estimate the symbol timing and carrier frequency errors. In order to improve the estimator performance, the correlation function is averaged on several OFDM symbols. However, the number of OFDM symbols in the averaging must be limited in order to reduce the interference caused by the clock frequency error.
With this method, the obtained estimate of the carrier frequency error presents an ambiguity. Indeed, this error is composed of an integer number of subcarrier spacing added to a fractional part of this spacing. Only the second component can be recovered by the cross correlation estimation method. To estimate the integer number of subcarrier spacing involved in the carrier frequency error, a pilot symbol is required [9]. Subcarriers are retrieved without ambiguity at the FFT output by comparing the expected pilot with the received one.

3.3 Fine synchronization

3.3.1 Symbol timing tracking

Plotted as a function of the subcarrier index n, the phase errors $\{\theta_{i,n}\}_{n=-\frac{N}{2},\ldots,\frac{N}{2}-1}$ for the i-th OFDM symbol are distributed on a line, the slope of which is proportional to τ (see equation 7). Assuming that interferences have been sufficiently reduced by the coarse synchronization stage, τ can be estimated from the set $\{Y_{i,n}^4\}_{n=-\frac{N}{2},\ldots,\frac{N}{2}-1}$, when the data transmitted on the subcarriers are mapped onto a QPSK constellation (the fourth power is used to remove the modulation) [10].

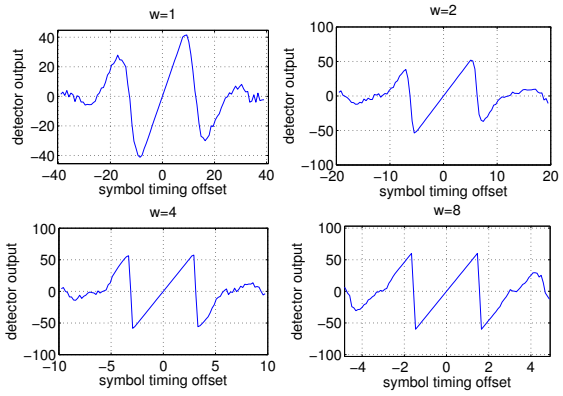

Figure 2: S-curves plotted for different values of w as a function of the symbol timing error value in percentage of N (no noise, no cyclic prefix).

Moreover, as illustrated on figure 1, an additional pre-averaging operation [10]:

$$Q_p = \frac{1}{w}\sum_{k=0}^{w-1} Y_{i,k-N/2+pw}^4 \qquad (8)$$

allows to estimate the slope with more accuracy. Parameter w is adjustable. Increasing w leads to a smaller estimation variance but also a smaller loop acquisition range (see figure 2).
On figure 2, acquisition ranges of the symbol timing loop have been obtained without cyclic prefix. For each value of w, adding this length to the cyclic prefix duration leads to the length of the interval I_{th} in which the residual symbol timing error has to be included after coarse synchronization.

3.3.2 Frequency carrier tracking

Plotted as a function of the subcarrier index n, the set of phase errors $\{\theta_{i,n} - \theta_{i-1,n}\}_{n=-\frac{N}{2},\ldots,\frac{N}{2}-1}$ affecting two consecutive OFDM symbols are distributed on a line whose value for $n = 0$ is proportional to Δf (see equation 7). Assuming that interferences have been sufficiently reduced by the coarse synchronization stage, Δf can be estimated by averaging the angles of $(Y_{i,n}Y_{i-1,n}^*)^4$, leading to $\{\theta_{i,n} - \theta_{i-1,n}\}$, on the N possible values for n (see figure 1) [5].
Figure 3 displays the S-curves of the carrier frequency detector for different values of $Eb/N0$. QPSK modulation is considered on each subcarrier.

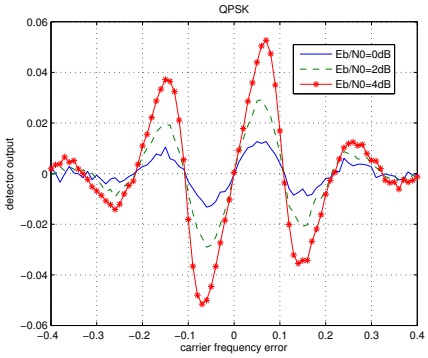

Figure 3: S-curves plotted for different values of $Eb/N0$ as a function of the carrier frequency error value in percentage of inter-carrier spacing.

These S-curves give the interval f_{th} in which the residual carrier frequency error has to be included after coarse synchronization : $|\Delta f|$ has to be lower than 11.5% of the subcarrier spacing whatever is $Eb/N0$.

3.3.3 Carrier phase tracking

In order to retrieve the emitted symbols, the carrier phase error must be corrected on each subcarrier. A loop is used for that purpose with the following phase detector [11], [12]:

$$P_{i,n} = sgn\left[\Im(Y_{i,n})\right]\left[\Re(\widehat{X_{i,n}}) - \Re(Y_{i,n})\right] - sgn\left[\Re(Y_{i,n})\right]\left[\Im(\widehat{X_{i,n}}) - \Im(Y_{i,n})\right], \qquad (9)$$

where sgn stands for the sign function and $\widehat{X_{i,n}}$ is the decided symbol from received $Y_{i,n}$.

4. SIMULATION RESULTS

4.1 Coarse synchronization

The goal of the coarse synchronization stage is to obtain low enough residual symbol timing and carrier frequency error to allow the convergence of the loops in the fine synchronization stage. "Low enough" means here that the residual symbol timing error and the residual carrier frequency error have respectively to be included in I_{th} (see section 3.3.1) and f_{th} (see section 3.3.2).
A study of the coarse synchronization performance is investigated in [13]. Proposed receiver parameters have been optimized in order to reach coarse synchronization objectives while providing a best spectral efficiency compared to single carrier systems such as DVB-S and DVB-S2.

4.2 Fine synchronization

We assume that the coarse synchronization stage has been properly performed (as described in previous section).
We first evaluate the performance of the joint symbol timing and carrier frequency locked loop. Considered parameters are: $N = 512$, QPSK mapping on each subcarrier and $w = 4$. Figure 4 displays the standard deviation for the residual symbol timing error as a function of $Eb/N0$, for different value of the noise bandwidth B_lT.

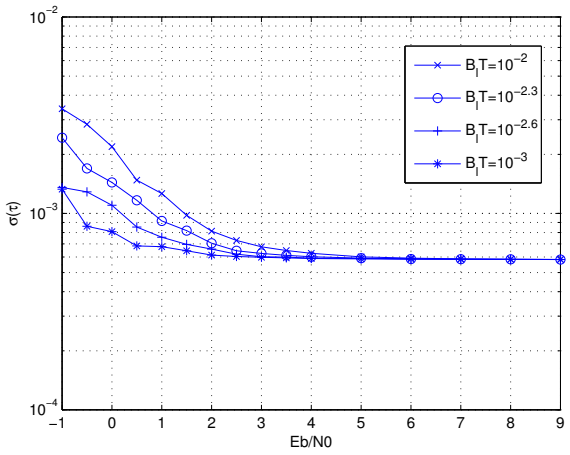

Figure 4: Performance of fine symbol timing synchronization.

After fine symbol timing synchronization, the symbol timing error standard deviation is lower than 0.4% of the OFDM symbol duration. This jitter, combined with coarse synchronization performance on the cyclic prefix length [13], allows to verify condition $-Np < \tau \leq 0$ after fine synchronization. So, Inter Symbol Interference is eliminated (see 2.1).
As illustrated on figure 4, the standard deviation of the residual symbol timing error reaches a plateau for high values of $Eb/N0$. This plateau is due to the quantization performed in the symbol timing error correction stage. The quantization step is equal to one sample of the OFDM symbol leading to a uniform quantization noise whose standard deviation σ is:

$$\sigma = \frac{1}{2\sqrt{3}N} \approx 5.6 \times 10^{-4} \qquad (10)$$

When oversampling is used to remove the quantization effect, there is no more plateau (see figure 5).

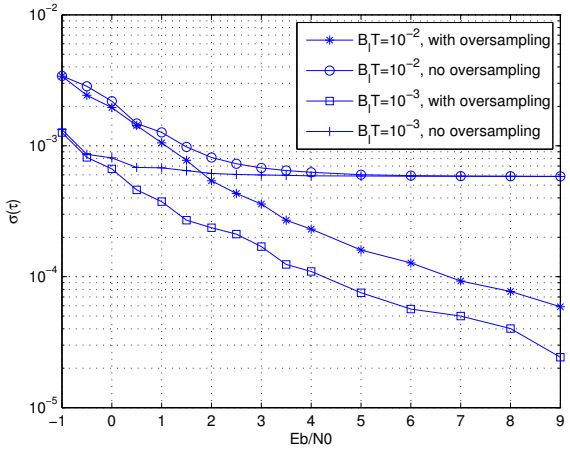

Figure 5: Performance of fine symbol timing synchronization with oversampling operation.

Figure 6 plots the performance of the symbol timing synchronization loop as a function of $Eb/N0$ for different values of w. A loop bandwidth B_lT of 10^{-2} is considered.
The performance of the symbol timing loop increases with w. But increasing w leads to a smaller loop acquisition range of the symbol timing loop. In that case, the accuracy of the coarse synchronization stage has to be improved, leading to consider a longer cyclic prefix which reduces system spectral efficiency. A trade off on the value of w has to be performed [13].

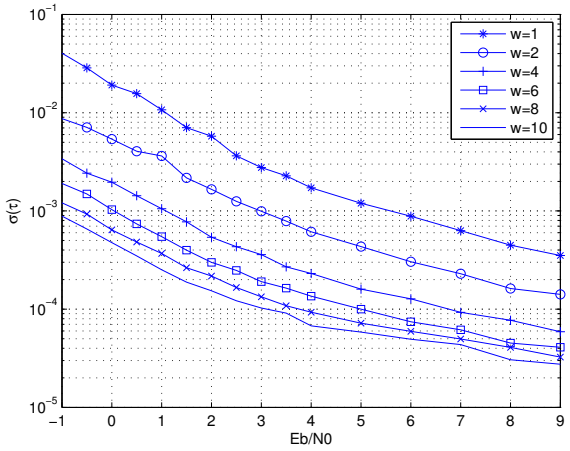

Figure 6: Performance of fine symbol timing synchronization as a function of w.

Figure 7 plots the standard deviation of the residual carrier frequency error as a function of $Eb/N0$, for different values of B_lT. A jitter lower than 2% of subcarrier spacing is obtained, leading to a performance degradation lower than $0.3dB$, at $BER = 10^{-4}$ (based on [7]).

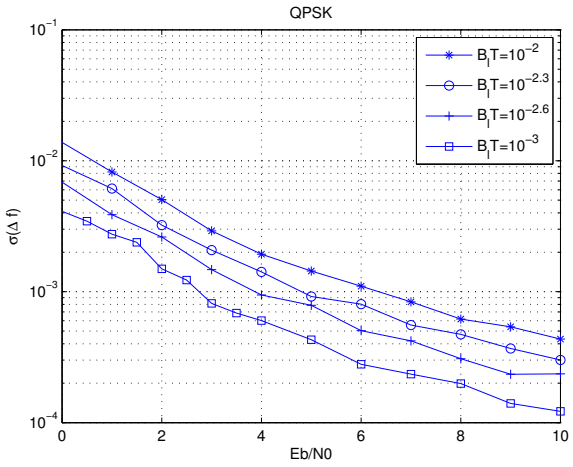

Figure 7: Performance of fine carrier frequency synchronization.

Finally, carrier phase correction is performed with a DPLL on each subcarrier. It is important to note that residual symbol timing and carrier frequency errors induce a phase noise at the input of this DPLL (see equation 7).

Figure 8 displays the standard deviation of the residual carrier phase error averaged on N subcarriers, as a function of noise bandwidth B_lT. Different values of $Eb/N0$ are considered. As expected, we can observe the classical trade off to be performed on B_lT value: phase jitter due to thermal noise increases with B_lT whereas phase jitter due to residual phase noise decreases with B_lT.

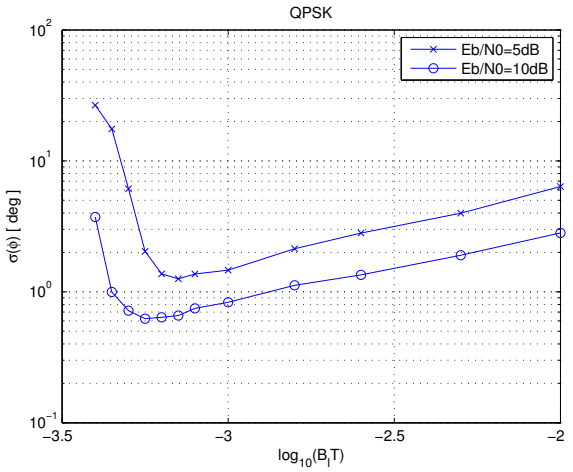

Figure 8: Final receiver performance for QPSK mapping on each subcarrier.

However, the phase noise due to residual carrier frequency and symbol timing errors at the input of the carrier phase locked loop is different on each subcarrier (see equation 7). As a consequence, the residual jitter at the output of the carrier phase locked loop is different on each subcarrier. This dependance on n leads to optimize B_lT on each subcarrier.

5. CONCLUSION

This paper addresses the performance of an OFDM receiver to be used on a non frequency selective channel. The receiver synchronization structure is presented. The idea is to reduce the overhead, compared to terrestrial systems using OFDM waveform, in order to reach a high spectral efficiency. Indeed, the satellite channel being non frequency selective, there is no need neither for cyclic prefix (no ISI) or for channel estimation pilots. Our receiver is based on non pilot aided algorithms involving feedback retroaction and relying on a first coarse synchronization stage using a reduced overhead. Several simulations showed the performance of the proposed receiver. Perspectives include the optimization of the noise bandwidth on each subcarrier, leading to the improved performance of the overall system.

REFERENCES

[1] M. Morelli, C.-C. Kuo, and M.-O. Pun, "Synchronization techniques for orthogonal frequency division multiple access (ofdma): A tutorial review," *Proceedings of the IEEE*, vol. 95, no. 7, pp. 1394 – 1427, July 2007.

[2] B. Ai and al, "On the synchronization techniques for wireless ofdm systems," *IEEE Transactions on Broadcasting*, vol. 52, no. 2, pp. 236 – 244, June 2006.

[3] S. A. Fechtel, "Ofdm carrier and sampling frequency synchronization and its performance on stationary and mobile channels," *IEEE Transactions on Consumer Electronics*, vol. 46, no. 3, pp. 438–441, Aug. 2000.

[4] V. Lottici, A. D'Andrea, and U. Mengali, "A new frequency loop for ofdm systems," *IEEE Transactions on Consumer Electronics*, vol. 46, no. 4, pp. 970–979, Nov. 2000.

[5] H. Roh and K. Cheun, "Non-data-aided spectral-line method for fine carrier frequency synchronization in ofdm receivers," *Journal of Communications and Networks*, vol. 6, no. 2, June 2004.

[6] B. Yang and al., "Timing recovery for ofdm transmission," *IEEE J. Sel. Areas Comm.*, vol. 18, no. 11, pp. 2278–2291, Nov. 2000.

[7] T. Pollet, M. V. Bladel, and M. Moeneclaey, "Ber sensitivity of ofdm systems to carrier frequency offset and wiener phase noise," *IEEE Trans. Comm.*, vol. 43, pp. 191–193, 1995.

[8] J. J. V. de Beek, M. Sandelland, and P. O. Brjesson, "Ml estimation of time and frequency offset in ofdm systems," vol. 45, no. 7, pp. 1800–1805, July 1997.

[9] M. Schmidl and D. C. Cox, "Robust frequency and timing synchronization for ofdm," *IEEE Transactions on Communications*, vol. 45, no. 12, pp. 1613–1621, Dec. 1997.

[10] D. Lee and K. Cheun, "A new symbol timing recovery algorithm for ofdm systems," *IEEE Transactions on Consumer Electronics*, vol. 43, no. 3, pp. 767–775, June 1997.

[11] A. Leclert and P. Vandamme, "Universal carrier recovery loop for qask and psk signals sets," *IEEE Trans. Comm.*, vol. 31, no. 1, pp. 130–136, Jan. 1983.

[12] A. Metref, D. L. Guennec, and J. Palicot, "Optimized decision-directed carrier recovery loop for 16-qam constellations," in *Proc. IEEE Global Com. Conf. (GLOBECOM)*, Washington, USA, Nov. 2007, pp. 3112–3117.

[13] A. T. Ho and al., "Ofdm synchronization scheme for the forward link of a fixed broadband satellite system," *9th IEEE SPAWC, Workshop Signal Processing Advances Wireless Comm.*, Recife, Brazil, July 6-9, 2008, paper to appear.